

A widely tunable 10- μm quantum cascade laser phase-locked to a state-of-the-art mid-infrared reference for precision molecular spectroscopy

P.L.T. Sow,^{1,2} S. Mejri,^{2,1} S.K. Tokunaga,^{2,1} O. Lopez,^{1,2} A. Goncharov,^{2,1, a)} B. Argence,^{1,2} C. Chardonnet,^{1,2} A. Amy-Klein,^{2,1} C. Daussy,^{2,1} and B. Darquie^{1,2, b)}

¹⁾ CNRS, UMR 7538, LPL, 93430 Villetaneuse, France

²⁾ Université Paris 13, Sorbonne Paris Cité, Laboratoire de Physique des Lasers, 93430 Villetaneuse, France

We report the coherent phase-locking of a quantum cascade laser (QCL) at 10- μm to the secondary frequency standard of this spectral region, a CO₂ laser stabilized on a saturated absorption line of OsO₄. The stability and accuracy of the standard are transferred to the QCL resulting in a line width of the order of 10 Hz, and leading to our knowledge to the narrowest QCL to date. The locked QCL is then used to perform absorption spectroscopy spanning 6 GHz of NH₃ and methyltrioxorhenium, two species of interest for applications in precision measurements.

With their rich internal structure, molecules can play a decisive role in precision tests of fundamental physics. They are being used to test fundamental symmetries such as parity¹⁻³ or parity and time reversal⁴, to measure absolute values of fundamental constants⁵⁻⁷ and their possible temporal variation⁸⁻¹⁰. Many of these experiments can be cast as measurements of resonance frequencies of molecular transitions, for which ultra-stable and accurate sources in the mid-infrared (mid-IR) are highly desirable, since most rovibrational transitions are to be found in that region.

Our group has a long-standing interest in performing spectroscopic precision measurements on molecules at extreme resolutions around 10 μm ^{1,9,11}. We are currently working on two such measurements: the determination of the Boltzmann constant, k_B , by Doppler spectroscopy of ammonia^{6,12} and the first observation of parity violation by Ramsey interferometry of a beam of chiral molecules^{3,13}. For these experiments, we currently use spectrometers based on custom built ultra-stable CO₂ lasers. We obtain the required metrological frequency stability and accuracy — 10 Hz line width, 1 Hz stability at 1 s, accuracy of a few tens of hertz^{14,15} — by stabilizing these lasers to saturated absorption lines of molecules such as OsO₄. CO₂ lasers have a major shortcoming: a lack of tunability. They emit at CO₂ molecular resonances. An emission line is found every 30 to 50 GHz in the 9-11 μm wavelength range, and each line is tunable over about 100 MHz. Although, as in our spectrometers, this range can be extended a few gigahertz using electro-optical modulators (EOMs), this is done at the expense of power (EOMs at these wavelengths have an efficiency of 10⁻⁴) and necessitates subsequent spectral filtering. Overcoming these difficulties without the loss of stability is key to enabling precision measurements in the mid-IR.

One solution would be to use frequency comb-referenced continuous-wave (cw)¹⁶⁻¹⁸ or femtosecond¹⁹

mid-IR sources. These are based on frequency mixing in nonlinear crystals and provide absolute-frequency referencing, reasonable line widths and tunability, but are very complex and often exhibit limited power. By comparison, cw quantum cascade lasers (QCLs) are a new mature and robust technology that offer broad and continuous tuning over several hundred gigahertz at 100 mW-level powers. Several can be combined giving access to the whole mid-IR region. Recent studies of the emission spectrum of cw free-running distributed-feedback (DFB) QCLs²⁰⁻²⁴ confirm their suitability for high resolution spectroscopy and frequency metrology. Furthermore, narrow-emission, absolutely referenced mid-IR QCLs have been demonstrated, either by phase-locking to a CO₂ laser^{25,26}, frequency locking to a sub-Doppler molecular transition²⁷, optical injection locking²⁸ or phase-locking^{24,29,30} to narrow optical frequency comb-based sources. Sub-kHz emission line widths, corresponding to relative stabilities in the high 10⁻¹³, and accuracies of a few 10⁻¹² have been shown³⁰. Note however that most of this work has been done using QCLs emitting around 4-5 μm . Work at longer wavelengths (including most of the molecular fingerprint region) has remained scarce (see refs.²⁴⁻²⁶ around 9 μm).

We extended this range to 10 μm . A 10 μm QCL exhibiting remarkably low free-running frequency noise is coherently phase-locked to the OsO₄-stabilized CO₂ laser. This allows both line width narrowing, by about 4 orders of magnitude down to an unprecedented 10 Hz-level, and absolute frequency referencing at the 10⁻¹² level. In order to preserve some of its tunability, the QCL is in fact locked to one of two optical sidebands (tunable over 10 GHz) generated by coupling the CO₂ laser light through an EOM. Once locked, we use this QCL to demonstrate high-resolution spectroscopy of both NH₃ and methyltrioxorhenium (MTO) over a range of over 6 GHz. These species are of interest for the two precision measurements under progress in our group. The former is our molecule of choice for measuring k_B , while the latter, MTO is an achiral test organometallic complex whose chiral derivatives are considered for a parity violation test^{3,13,31}.

^{a)}Permanent address: Institute of Laser Physics of SB RAS, Pr. Lavrentyeva 13/3, Novosibirsk, 630090 Russia

^{b)}Electronic mail: benoit.darquie@univ-paris13.fr

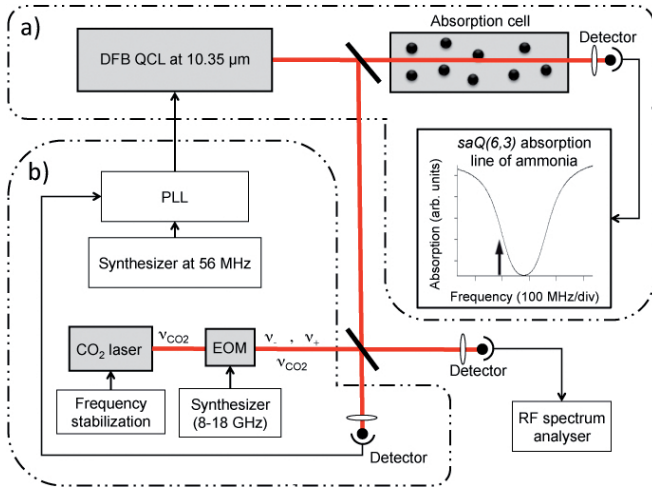


FIG. 1. Sketch of the experimental setup. (a) Two different absorption of 5 cm and 60 cm-path length cells are respectively used for the free-running QCL frequency noise analysis and for high resolution spectroscopy. The graph shows the measured $saQ(6,3)$ rovibrational line of the ν_2 vibrational mode of $^{14}\text{NH}_3$ used as frequency discriminator (250 Pa) recorded with our ultra-stable CO_2 laser based spectrometer³². The abscissa shows the detuning from the line center (28 953 693.9(1) MHz). The arrow represents the QCL operating point when recording the frequency noise power spectral density shown in Fig. 2. (b) Setup used to coherently phase-lock the QCL to a frequency-stabilized CO_2 laser. QCL: quantum cascade laser, DFB: distributed-feedback, EOM: electro-optic modulator.

The QCL is a cw-mode near-room-temperature (near-RT) single-mode DFB laser (from Alpes Lasers) tunable between 10.34 and 10.42 μm (28.76 to 29.00 THz). For the experiments described in this paper, it is typically operated at a temperature of 243 K (at which the threshold current is 710 mA) and a current ranging from 0.96 to 1.02 A, delivering 40 to 60 mW around 28.95 THz. At the QCL output, the laser beam is collimated with a spherical ZnSe lens ($f = 25$ mm). First, we measure the frequency noise of the free-running QCL. This allows us to estimate the feedback bandwidth required to narrow its line width. As illustrated in Fig. 1(a), we use the side of an ammonia linear absorption line as frequency discriminator. The absorption signal from a 5 cm path length cell containing 250 Pa of NH_3 is recorded with a liquid nitrogen-cooled HgCdTe detector (with a bandwidth of a few megahertz) and processed by a Fast Fourier Transform (FFT) spectrum analyzer. The frequency-to-amplitude conversion coefficient is measured by recording the same rovibrational line using our stabilized CO_2 laser spectrometer³². Fig. 2 shows the resulting frequency noise power spectral density (PSD) of the QCL. It has a $1/f$ trend at low frequency, followed by a steeper slope above ~ 300 kHz, as observed in^{21,22}. Note however that the measured frequency noise PSD is roughly one order of magnitude lower than previously published characterizations of free-running cw-mode near-RT DFB QCLs²⁰⁻²⁴.

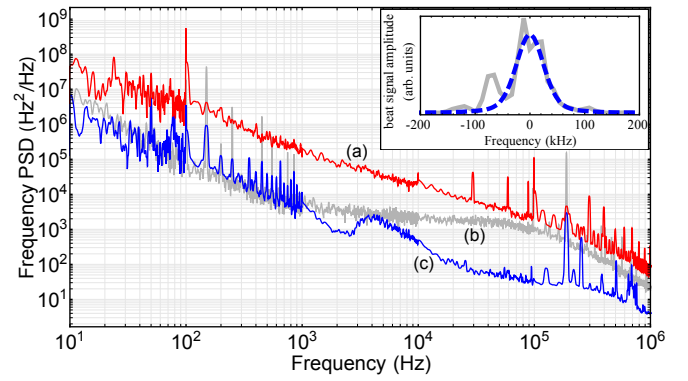


FIG. 2. Frequency noise PSD of the 10.35 μm DFB QCL (red line (a)). The contributions of the laser intensity noise (blue line (c)) and laser driver current noise (green line (b)) are also plotted for comparison. The inset shows the beat signal between the QCL and the sideband of a ~ 1 kHz wide free-running CO_2 laser recorded with a RF spectrum analyzer (1 kHz resolution bandwidth). The dashed line is the QCL line shape calculated from the measured frequency noise PSD. For these measurements the QCL was conveniently locked to the side of the $saQ(6,3)$ NH_3 line with a ~ 1.5 Hz bandwidth.

Fig. 2 also shows the contribution from the laser intensity noise, obtained with the laser tuned far off resonance, as well as the contribution from a home-made low-noise current source. The latter is obtained by multiplying the driver's current noise spectrum (< 300 pA/ $\sqrt{\text{Hz}}$ above 10 kHz) by the laser DC current-to-frequency response (230 MHz/mA). The driver's current noise was accurately measured by balancing two identical home-made sources of opposite polarity and detecting the residual AC-currents.

Fig. 2 also shows that the expected white noise level N_w corresponding to the Schawlow-Townes limit does not seem to be reached at 1 MHz. Thus, only an upper limit of $N_w \sim 50$ Hz²/Hz (and an upper limit of the corresponding intrinsic laser line width of $\Delta\nu = \pi N_w \sim 160$ Hz) can be inferred. This is 1.7 times lower than measured for a cw mode near-RT DFB QCL at 4.3 μm ²³.

The real laser line width is broadened by flicker noise and depends on the observation time. The inset in Fig. 2 shows a beat signal between the free-running QCL and a free-running CO_2 laser which exhibits a record ~ 60 kHz full width at half maximum after 1 ms of integration time (*i.e.* 1 kHz resolution bandwidth). The line width of the free-running CO_2 laser was measured to be ~ 1 kHz³³, making its contribution negligible in the observed width. The measured beat signal agrees well with a theoretical estimation of the QCL emission line shape based on the measured frequency noise PSD (following³⁴ and accounting for the 1 ms observation time³⁵) as indicated by the dashed line in the inset of Fig. 2.

The experimental setup used to coherently phase-lock the QCL to a CO_2 laser stabilized on a saturated absorption line of OsO_4 is shown on Fig. 1(b). In this work, the $R(6)$ CO_2 laser carrier is frequency-locked to the

$R(23)A_1^1(-)$ line of $^{192}\text{OsO}_4$. Once stabilized, light from the CO_2 laser is coupled to an EOM which generates two sidebands of frequencies $\nu_{\pm} = \nu_{\text{CO}_2} \pm f_{\text{EOM}}$ on either side of the fixed laser frequency ν_{CO_2} . The frequency f_{EOM} is tunable from 8 to 18 GHz. The QCL ($\sim 100 \mu\text{W}$) and the CO_2 laser beams are overlapped and the beat signal is detected by a liquid nitrogen-cooled HgCdTe detector with a bandwidth of about 100 MHz. With a $\sim 10^{-4}$ EOM efficiency, $\sim 1 \mu\text{W}$ ($\sim 10 \text{ mW}$) is available for the beat signal in each of the CO_2 laser sidebands (in the carrier).

The phase-error signal is generated by comparing the phase of the amplified (60 dB) beat signal with a synthesized reference signal typically at 56 MHz using a frequency mixer. A phase-lock servo loop is used to apply a correction signal directly to the QCL's current.

The beat spectrum between a CO_2 laser sideband and the QCL phase-locked to this sideband, processed by a radio-frequency (RF) spectrum analyzer, is shown in Fig. 3(a). It is recorded with a second out-of-loop photodetector (see Fig. 1), similar to the one in-loop, in order to avoid errors brought by the detection setup and associated electronics. It represents the relative phase noise spectral density between the QCL and the CO_2 laser. With a typical signal-to-noise ratio of 60 dB in a 30 kHz resolution bandwidth we achieve a feedback bandwidth between 1 and 3 MHz (as indicated by the servo-loop unity gain frequency bump in the spectrum wings). As expected for a proper phase-lock, the beat signal of Fig. 3(a) exhibits an extremely narrow central peak. Its width was observed to be limited by the 10-Hz resolution of our RF spectrum analyzer. Fig. 3(b) shows the phase-noise power spectral density of the beat-signal between the CO_2 laser carrier and the phase-locked QCL (the beat signal of the out-of-loop photodetector is down-mixed to DC and processed with a FFT spectrum analyzer). The phase-lock performance can be characterized by the residual rms phase error, σ_{φ} . Integration of the phase-noise data in Fig. 3(b) from 1 Hz up to 5 MHz leads to a very small $\sigma_{\varphi} \sim 0.017$ rad, corresponding to having $e^{-\sigma_{\varphi}^2} \sim 99.97\%$ of the beat signal RF power concentrated in the coherent part (*i.e.* in the central peak)³⁶.

This is a signature of a highly coherent phase-lock and of the excellent transfer of the locked CO_2 laser's spectral features to the QCL. This results in a record QCL line width of the order of 10 Hz, 3 to 4 orders of magnitude lower than a free-running QCL, and a relative stability at 1 s of about 1 Hz. Our particular choice of OsO_4 line for absolute frequency referencing leads to a 90 Hz accuracy of the frequency scale^{15,37}. To our knowledge, this is the first demonstration that a QCL can reach these metrological spectral properties.

Linear absorption spectra of both NH_3 and MTO are shown on Fig. 4. The setup has been described above, and is depicted in Fig. 1. A few-millimeter wide beam of $1 \mu\text{W}$ is sent through a 60-cm long cell filled with either $\sim 10 \text{ Pa}$ of ammonia or $\sim 4 \text{ Pa}$ of MTO. A slotted disk, that chops the beam at 2 kHz, and a lock-in detection are

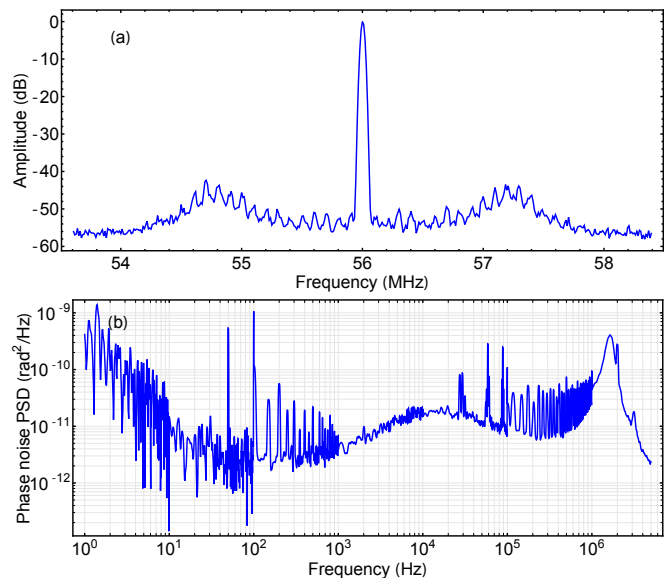


FIG. 3. (a) Beat signal spectrum between the frequency-stabilized CO_2 laser sideband and the phase-locked QCL taken with a RF spectrum analyzer (30 kHz resolution bandwidth). (b) Phase-noise power spectral density of the beat signal between the QCL and the frequency-stabilized CO_2 laser carrier.

used for noise filtering. The QCL is phase-locked to the EOM's negative sideband (frequency ν_-), red-detuned from the CO_2 laser carrier (frequency ν_{CO_2}). Sweeping the EOM frequency enables us to continuously tune the QCL over ~ 6 GHz, more than 10^8 times the laser line width. With a few milliwatts available for spectroscopy, this also results in an effective power amplification of $\sim 10^3$ compared to using the CO_2 laser beam's negative sideband directly. The ammonia spectrum in Fig. 4 exhibits three isolated rovibrational lines of the ν_2 vibrational mode of $^{14}\text{NH}_3$. The MTO spectrum looks very different with a mean $\sim 5.5\%$ absorption and ~ 100 MHz wide $\sim 2\%$ deviations as expected from the dense anti-symmetric $\text{Re}=\text{O}$ stretching mode of the molecule^{3,13,31}. Both spectra were normalized by numerically correcting for the baseline.

In conclusion we characterized the frequency noise of a free-running cw near-RT DFB $10.3 \mu\text{m}$ QCL. The laser is then phase-locked to a frequency-stabilized CO_2 laser, and we observe that the spectral properties of the latter are successfully copied to the QCL. This results in a record line width of the order of 10 Hz, a relative stability at 1 s in the 10^{-14} range and a relative accuracy of 3×10^{-12} . Spectra of ammonia and MTO over several GHz using our QCL source were presented, thereby demonstrating the potential of QCLs for precision measurements devoted to metrological applications or tests of fundamental laws of nature.

The use of QCLs will eventually allow the study of any species showing absorption between 3 and $25 \mu\text{m}$, with much broader continuous tuning range and with

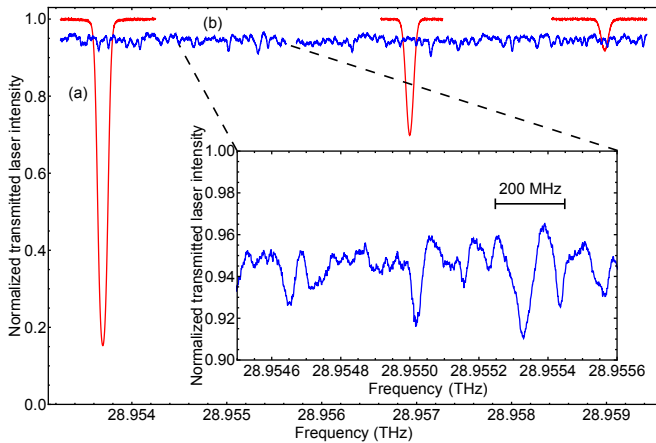


FIG. 4. Linear absorption spectra of NH_3 (red curve (a)) and MTO (blue curve (b)) recorded over more than 6 GHz with a ~ 10 Hz line width QCL phase-locked to a frequency-stabilized CO_2 laser. From left to right, the ammonia spectrum exhibit the three isolated rovibrational lines $saQ(6,3)$ (probed in our experiment dedicated to the determination of k_B^6), $saQ(6,2)$ and $saQ(6,1)$ of the ν_2 vibrational mode of $^{14}\text{NH}_3$. The inset shows a zoom on the MTO spectrum. Experimental conditions: chopper frequency 2 kHz, lock-in amplifier time constant 30 ms, 500 kHz steps, power 1 μW , absorption length 60 cm, ~ 10 Pa of NH_3 or ~ 4 Pa of MTO.

reasonable powers. It will broaden the scope of our spectroscopic precision measurement experiments using molecules. We eventually plan to reach the 3×10^{-16} accuracy of the Cs fountain³⁸, the 10^{-15} stability of the best near-IR oscillators, and take full advantage of the QCL's tunability by locking it to a frequency comb stabilized via an optical fiber to an ultra-stable near-IR reference monitored against atomic fountain clocks. This was recently demonstrated in our group with a CO_2 lasers³⁹. Stabilizing the laser this way provides the ultimate frequency accuracy and stability, and frees us from having to lock the QCL to any particular reference (another laser or a molecular transition), which would constrain the laser's operating frequency. Finally, narrow line width light sources such as QCLs would benefit the entire spectroscopy community, beyond our scope of interest. Commercial QCLs are available at wavelengths spanning the entire mid-IR, the molecular fingerprint region, which hosts many spectral signatures of molecules of interest for atmospheric, planetary or interstellar physics, chemistry, biology, medical or industrial diagnostics.

The authors acknowledge financial support from CNRS, Université Paris 13, LNE, LabEx FIRST-TF (ANR-IO-LABX-48-01) and AS GRAM. This work is part of the projects NCPHEM n° 2010 BLAN 724 3 and QUIGARDE n° ANR-12-ASTR-0028-03 funded by the Agence Nationale de la Recherche (ANR, France).

¹C. Daussy, T. Marrel, A. Amy-Klein, C. T. Nguyen, C. Bordé, and C. Chardonnet, Phys. Rev. Lett. **83**, 1554 (1999).

- ²D. DeMille, S. B. Cahn, D. Murphree, D. A. Rahlmow, and M. G. Kozlov, Phys. Rev. Lett. **100**, 23003 (2008).
- ³B. Darquié, C. Stoeffler, A. Shelkovnikov, C. Daussy, A. Amy-Klein, C. Chardonnet, S. Zrig, L. Guy, J. Crassous, P. Soulard, P. Asselin, T. R. Huet, P. Schwerdtfeger, R. Bast, and T. Saue, Chirality **22**, 870 (2010).
- ⁴J. Baron, W. C. Campbell, D. DeMille, J. M. Doyle, G. Gabrielse, Y. V. Gurevich, P. W. Hess, N. R. Hutzler, E. Kirilov, I. Kozyryev, B. R. O'Leary, C. D. Panda, M. F. Parsons, E. S. Petrik, B. Spaun, A. C. Vutha, and A. D. West, Science **343**, 269 (2014).
- ⁵J. C. J. Koelemeij, B. Roth, A. Wicht, I. Ernsting, and S. Schiller, Phys. Rev. Lett. **98**, 173002 (2007).
- ⁶C. Lemarchand, S. Mejri, P. L. T. Sow, M. Triki, S. K. Tokunaga, S. Briau, C. Chardonnet, B. Darquié, and C. Daussy, Metrologia **50**, 623 (2013).
- ⁷L. Moretti, A. Castrillo, E. Fasci, M. D. De Vizia, G. Casa, G. Galzerano, A. Merlone, P. Laporta, and L. Gianfrani, Physical Review Letters **111**, 060803 (2013).
- ⁸E. R. Hudson, H. J. Lewandowski, B. C. Sawyer, and J. Ye, Phys. Rev. Lett. **96**, 143004 (2006).
- ⁹A. Shelkovnikov, R. J. Butcher, C. Chardonnet, and A. Amy-Klein, Phys. Rev. Lett. **100**, 150801 (2008).
- ¹⁰S. Truppe, R. J. Hendricks, S. K. Tokunaga, H. J. Lewandowski, M. G. Kozlov, C. Henkel, E. A. Hinds, and M. R. Tarbutt, Nature communications **4**, 2600 (2013).
- ¹¹M. Ziskind, C. Daussy, T. Marrel, and C. Chardonnet, The European Physical Journal D **20**, 219 (2002).
- ¹²C. Lemarchand, M. Triki, B. Darquié, C. J. Bordé, C. Chardonnet, and C. Daussy, New Journal of Physics **13**, 073028 (2011).
- ¹³S. K. Tokunaga, C. Stoeffler, F. Auguste, A. Shelkovnikov, C. Daussy, A. Amy-Klein, C. Chardonnet, and B. Darquié, Molecular Physics **111**, 2363 (2013).
- ¹⁴V. Bernard, C. Daussy, G. Nogues, L. Constantin, P. E. Durand, A. Amy-Klein, A. van Lerberghe, and C. Chardonnet, IEEE J. Quant. Elec. **QE-33**, 1282 (1997).
- ¹⁵O. Acef, F. Michaud, and G. V. Rovera, IEEE Transactions on Instrumentation and Measurement **48**, 567 (1999).
- ¹⁶I. Galli, S. Bartalini, S. Borri, P. Cancio, D. Mazzotti, P. De Natale, and G. Giusfredi, Phys. Rev. Lett. **107**, 270802 (2011).
- ¹⁷U. Bressel, I. Ernsting, and S. Schiller, Optics letters **37**, 918 (2012).
- ¹⁸I. Ricciardi, E. De Tommasi, P. Maddaloni, S. Mosca, A. Rocco, J.-J. Zondy, M. De Rosa, and P. De Natale, Opt. Express **20**, 9178 (2012).
- ¹⁹A. Schliesser, N. Picqué, and T. W. Hänsch, Nat. Phot. **6**, 440 (2012).
- ²⁰T. L. Myers, R. M. Williams, M. S. Taubman, C. Gmachl, F. Capasso, D. L. Sivco, J. N. Baillargeon, and a. Y. Cho, Optics letters **27**, 170 (2002).
- ²¹S. Bartalini, S. Borri, P. Cancio, a. Castrillo, I. Galli, G. Giusfredi, D. Mazzotti, L. Gianfrani, and P. De Natale, Physical Review Letters **104**, 083904 (2010).
- ²²L. Tombez, J. D. Francesco, S. Schilt, G. D. Domenico, J. Faist, P. Thomann, D. Hofstetter, J. Di Francesco, S. Schilt, G. Di Domenico, J. Faist, P. Thomann, and D. Hofstetter, Opt. Lett. **36**, 3109 (2011).
- ²³S. Bartalini, S. Borri, I. Galli, G. Giusfredi, D. Mazzotti, T. Edamura, N. Akikusa, M. Yamanishi, and P. De Natale, Opt. Express **19**, 17996 (2011).
- ²⁴A. A. Mills, D. Gatti, J. Jiang, C. Mohr, W. Mefford, L. Gianfrani, M. Fermann, I. Hartl, and M. Marangoni, Opt. Lett. **37**, 4083 (2012).
- ²⁵F. Bielsa, A. Douillet, T. Valenzuela, J.-P. Karr, and L. Hilico, Opt. Lett. **32**, 1641 (2007).
- ²⁶F. Bielsa, K. Djerroud, A. Goncharov, A. Douillet, T. Valenzuela, C. Daussy, L. Hilico, and A. Amy-Klein, J. Mol. Spec. **247**, 41 (2008).
- ²⁷F. Cappelli, I. Galli, S. Borri, G. Giusfredi, P. Cancio, D. Mazzotti, A. Montori, N. Akikusa, M. Yamanishi, S. Bartalini, and

- P. De Natale, *Opt. Lett.* **37**, 4811 (2012).
- ²⁸S. Borri, I. Galli, F. Cappelli, A. Bismuto, S. Bartalini, P. Cancio, G. Giusfredi, D. Mazzotti, J. Faist, and P. De Natale, *Opt. Lett.* **37**, 1011 (2012).
- ²⁹M. G. Hansen, I. Ernsting, S. V. Vasilyev, A. Grisard, E. Lallier, B. Gérard, and S. Schiller, *Optics express* **21**, 27043 (2013).
- ³⁰I. Galli, M. Siciliani de Cumis, F. Cappelli, S. Bartalini, D. Mazzotti, S. Borri, A. Montori, N. Akikusa, M. Yamanishi, G. Giusfredi, P. Cancio, and P. De Natale, *Appl. Phys. Lett.* **102**, 121117 (2013).
- ³¹C. Stoeffler, B. Darquié, A. Shelkovnikov, C. Daussy, A. Amy-Klein, C. Chardonnet, L. Guy, J. Crassous, T. R. Huet, P. Soulard, and P. Asselin, *Phys. Chem. Chem. Phys.* **13**, 854 (2011).
- ³²C. Lemarchand, K. Djerroud, B. Darquié, O. Lopez, A. Amy-Klein, C. Chardonnet, C. J. Bordé, S. Briaudeau, and C. Daussy, *International Journal of Thermophysics* **31**, 1347 (2010).
- ³³V. Bernard, P. E. Durand, T. George, H. W. Nicolaisen, A. Amy-Klein, and C. Chardonnet, *IEEE Journal of Quantum Electronics* **QE-31**, 1913 (1995).
- ³⁴D. Elliott, R. Roy, and S. Smith, *Phys. Rev. A* **26**, 12 (1982).
- ³⁵M. Bishof, X. Zhang, M. J. Martin, and J. Ye, *Physical Review Letters* **111**, 093604 (2013).
- ³⁶M. Zhu and J. L. Hall, *J. Opt. Soc. Am. B* **10**, 802 (1993).
- ³⁷C. Chardonnet, *Spectroscopie de saturation de hautes précision et sensibilité en champ laser fort. Applications aux molécules OsO₄, SF₆ et CO₂ et à la métrologie des fréquences*, Ph.D. thesis, Université Paris 13, Villetaneuse (1989).
- ³⁸J. Guéna, M. Abgrall, D. Rovera, P. Laurent, B. Chupin, M. Lours, G. Santarelli, P. Rosenbusch, M. Tobar, R. Li, K. Gibble, A. Clairon, and S. Bize, *IEEE transactions on ultrasonics, ferroelectrics, and frequency control* **59**, 391 (2012).
- ³⁹B. Chanteau, O. Lopez, W. Zhang, D. Nicolodi, B. Argence, F. Auguste, M. Abgrall, C. Chardonnet, G. Santarelli, B. Darquié, Y. Le Coq, and A. Amy-Klein, *New J. Phys.* **15**, 073003 (2013).